



## Randomly oriented twin domains in electrodeposited silver dendrites

EVICA R. IVANOVIĆ<sup>1\*</sup>, NEBOJŠA D. NIKOLIĆ<sup>2#</sup> and VELIMIR R. RADMILOVIĆ<sup>3\*\*</sup>

<sup>1</sup>Faculty of Agriculture, University of Belgrade, Nemanjina 6, Belgrade-Zemun, Serbia,

<sup>2</sup>ICTM – Institute of Electrochemistry, University of Belgrade, Njegoševa 12, P. O. Box 473,

11001 Belgrade, Serbia and <sup>3</sup>Faculty of Technology and Metallurgy, University of Belgrade,  
Karnegijeva 4, P. O. Box 3503, 11001 Belgrade, Serbia

(Received 6 March, revised 16 April, accepted 18 April 2014)

**Abstract:** Silver dendrites were prepared by electrochemical deposition. The structures of the Ag dendrites, the type of twins and their distribution were investigated by scanning electron microscopy (SEM), Z-contrast high angle annular dark field transmission electron microscopy (HAADF), and crystallographically sensitive orientation imaging microscopy (OIM). The results revealed that the silver dendrites were characterized by the presence of randomly distributed 180° rotational twin domains. The broad surface of dendrites was of the {111} type. The directions of growth of the main dendrite stem and all branches were of the <112> type.

**Keywords:** dendrite; silver; electrodeposition; twinning; scanning electron microscopy; high angle annular dark field microscopy; orientation imaging microscopy.

### INTRODUCTION

Dendritic growth is one of the most complex patterns that evolves through the dynamic processes of crystal growth and therefore has remained an active subject for experimental and theoretical studies for an extended period. During the past several decades, dendritic growth has attracted a large number of researchers in the broad areas of material science, condensed matter physics, fluid dynamics, applied mathematics, etc.<sup>1–3</sup> It has been regarded as a typical example of a variety of pattern formations in nature and technology. Among various metals, the preparation of Ag dendrites has been widely investigated because of their unique optical properties and potential applications in surface-enhanced

\*,\*\* Corresponding authors. E-mail: (\*)ivaeva@agrif.bg.ac.rs; (\*\*)VRRadmilovic@tmf.bg.ac.rs

# Serbian Chemical Society member.

doi: 10.2298/JSC140306045I

Raman spectroscopy (SERS),<sup>4,5</sup> catalysis,<sup>6,7</sup> sensors<sup>8</sup> and the fabrication of superhydrophobic surfaces.<sup>9</sup>

Several methods were explored to synthesize dendritic Ag structures, including electrochemical deposition,<sup>10</sup> the galvanic replacement reaction,<sup>4,11,12</sup> electroless deposition,<sup>10</sup> sonoelectrochemistry,<sup>13,14</sup> microwave irradiation,<sup>15</sup> hydrothermal reduction,<sup>6</sup> photoreduction<sup>16</sup> and the template method.<sup>17</sup> Electrochemical deposition has an advantage over the other methods because the driving force, *i.e.*, overpotential, is more controllable and is able to produce dendritic structures with high purity. Therefore, electrodeposition represents a powerful technique that provides versatility in tailoring the architecture of metals on the micro/nanoscale.

Several mechanisms, such as the diffusion-limited aggregation (DLA) model,<sup>18</sup> oriented attachment growth,<sup>19–21</sup> nanoparticle-aggregated self-assembly crystallization,<sup>22</sup> anisotropic crystal growth,<sup>23</sup> site-specific sequential nucleation,<sup>11,24</sup> multistep self-assembly process<sup>12</sup> and the cluster–cluster aggregation model (CCA) model,<sup>25</sup> were proposed to explain Ag dendritic growth in various systems. The electrochemical literature has defined the problem of roughening in electrodeposition.<sup>10</sup> Mullins–Sekerka linear stability analysis<sup>26</sup> and the Barton–Bockris dendrite-propagation model<sup>27</sup> are popular methods used to describe cathodic roughening and dendritic growth in electrochemical deposition. These commonly cited theories employ kinetic relationships that differ in mathematical form, but both contain the effects of surface tension and local concentration deviations induced by surface roughening.

However, intrinsic dendritic structures, *i.e.*, the appearance of well-defined and fairly regular branching and directions of growth, cannot be explained by the nonspecific models mentioned above. The twin plane reentrant edge (TPRE) mechanism or WHS model<sup>28,29</sup> is also a much-cited model of dendritic growth. In this mechanism, crystal growth arises through the formation of reentrant grooves at the intersection by the twin planes, which make this location a favorable site for nucleation. Based on this model, a dendrite is a twin crystal with at least one twin boundary, which extends throughout the dendrite and is parallel to the main dendrite plane.

The aim of this research effort was to investigate the role of twinning, the type and shape of twins, and the presence of twin domains and their distribution in silver dendrites obtained by electrochemical deposition.

## EXPERIMENTAL

The electrodeposition was realized using a typical set-up consisting of a platinum cathode with geometric surface area of 0.53 cm<sup>2</sup>. The reference and counter electrodes were of pure silver. The counter electrode was silver foil of surface area approximately 0.80 dm<sup>2</sup>, placed close to the cell walls. The reference electrode was a silver wire, the tip of which was positioned at a distance of ≈0.2 cm from the surface of the working electrode. The working

electrode was placed in the center of the cell. The electrolyte solution consisted of 0.06 M AgNO<sub>3</sub> + 1.2 M NaNO<sub>3</sub> + 0.05 M HNO<sub>3</sub>. Double distilled water was used for preparing the solutions. The total electrolyte volume was 100 mL and the electrodeposition was performed at 100 mV, at room temperature. The electrodeposition time was 72 s. The as-prepared Ag dendrites were sequentially rinsed with distilled water and ethanol for further characterization.

The morphology and microstructure of silver dendrites were characterized and analyzed by SEM and crystallographically sensitive orientation imaging microscopy (OIM) using a DB235 FIB system, and by Z-contrast high angle annular dark field transmission electron microscopy (HAADF) using a TEAM 0.5 transmission electron microscope operating at 300 kV. Orientation imaging microscopy (OIM) is based on electron-backscattered diffraction (EBSD), generated from the top 10 to 50 nm of the material surface. When exposed to the atmosphere, silver dendrites can rapidly oxidize, covering the surface with Ag<sub>2</sub>O. A silver oxide film would decrease the signal to noise ratio and make it difficult to analyze silver dendrite twin structures using the EBSD tool. To solve this problem, Ferrer *et al.*<sup>30</sup> proposed the solution of having an EBSD system installed on a dual-beam focused ion beam system (FIB). This concept allows the EBSD analysis to be performed immediately after material surface preparation,<sup>31</sup> using a focused ion beam (FIB), without breaking the vacuum.

## RESULTS AND DISCUSSION

The polarization curve for silver electrodeposition from 0.06 M AgNO<sub>3</sub> + 1.2 M NaNO<sub>3</sub> + 0.05 M HNO<sub>3</sub> is shown in Fig. 1a. The plateau of the limiting diffusion current density corresponds to the range of overpotentials between 75 and 175 mV. The dependence of the current density on the time of electrodeposition obtained at an overpotential of 100 mV is presented in Fig. 1b. A fast increase in the current density with electrodeposition time was observed during the electrodeposition process at this overpotential.

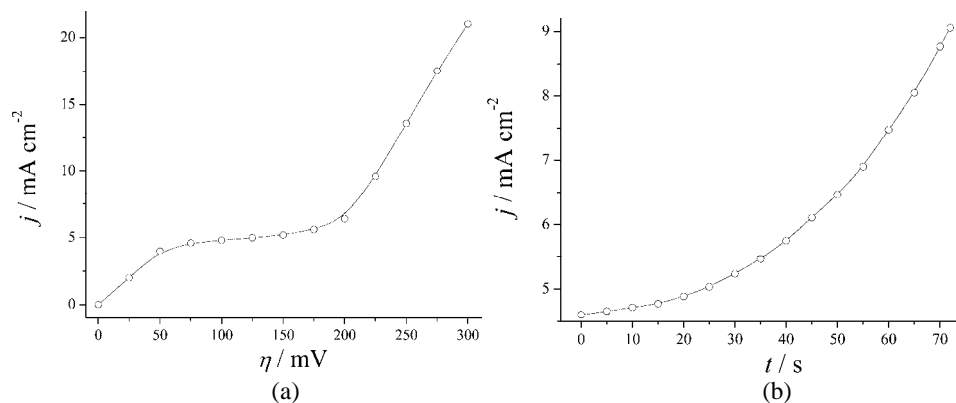


Fig. 1. a) Polarization curve for silver electrodeposition from 0.06 M AgNO<sub>3</sub> + 1.2 M NaNO<sub>3</sub> + 0.05 M HNO<sub>3</sub>. b) Dependence of the current density on the time of electrodeposition obtained at an overpotential of 100 mV. The electrodeposition time was 72 s.

The typical morphology of electrodeposited silver dendrites obtained at an overpotential of 100 mV, characterized by scanning electron microscopy (SEM),

is shown in Fig. 2a. The simplest dendrites consisted of only the stem and primary branches and are referred to as primary (P) dendrites. If the primary branches in turn developed secondary branches, the dendrites are called secondary (S). With an additional set of branches, tertiary (T) dendrites were formed.

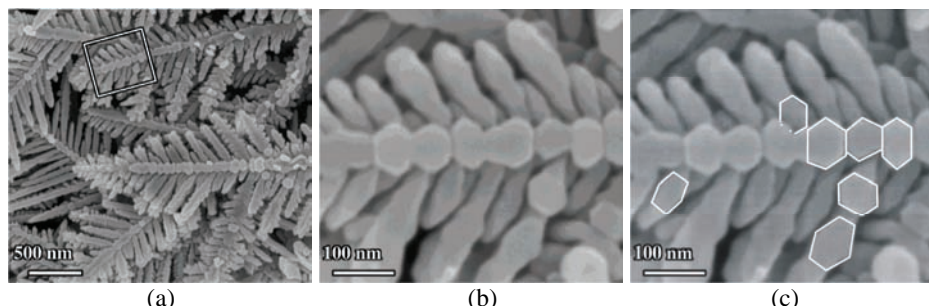


Fig. 2. a) Scanning electron micrograph of electrodeposited silver dendrites. b) Enlarged detail (see rectangle in a) showing twinned (stacked) octahedrons in the dendrite stem. c) Drawing indicating how Ag dendrite stems and branches are formed by the stacking of hexagonal units.

From the SEM image, it appears that these dendrites were two-dimensional patterns with the main stem and all branches being in the same plane; such dendrites are often referred to as two-dimensional or 2D crystals.<sup>32</sup> Figure 2b shows that the main stem of a dendrite is formed by the stacking of octahedrons mostly in the elongated form undergoing longitudinal propagation along the specific crystallographic direction. Primary and secondary hexagons (mostly irregular) develop and grow outwards from the main stem, as is shown in Fig. 2c.

A high angle annular dark field (HAADF) transmission electron micrograph of a silver dendrite is shown in Fig. 3. Both, the primary and secondary branches exhibited much the same or similar contrast, indicating they were all of approximately the same or similar thicknesses. The exceptions are the bright dots on the main stem, which indicate that some of the primary branches had grown perpendicular to the main stem and to the broad main dendrite surface.

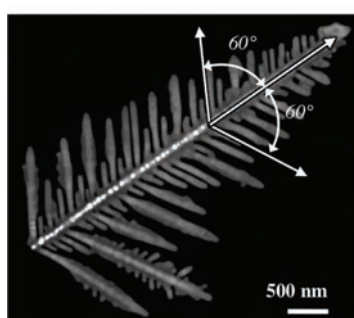


Fig. 3. High angle annular dark field (HAADF) transmission electron micrograph of silver dendrite showing the angles between the stem and the branches.

The angles between the main stem and primary branches, as well as between primary and secondary branches were  $60^\circ$ . This angular relationship between branches indicates that the main axis of the dendrite was parallel to the  $\langle 112 \rangle$  direction and all branches were also parallel to the same family of crystallographic directions.

A 100 pole figure of an Ag dendrite is shown in Fig. 4a. From this pole figure, it is obvious that the crystallographic orientation of this silver dendrite was close to 111, indicated by the 111 pole being in the center of the stereographic projection. There are two sets of 100 poles present in this pole figure, related to each other by rotation of  $180^\circ$  around the [111] direction.

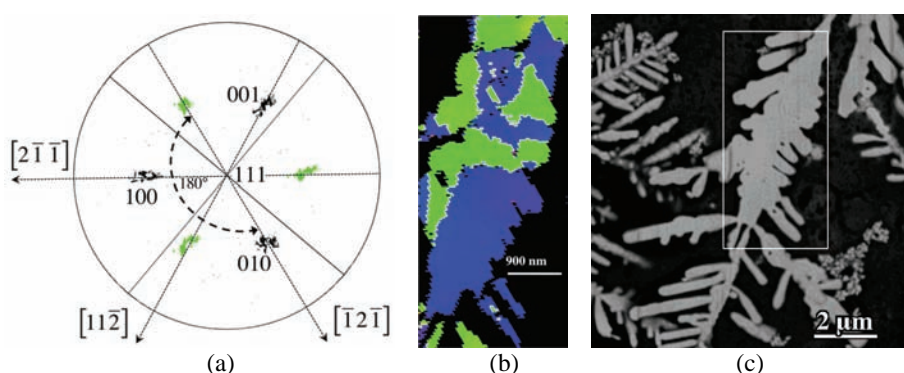


Fig. 4. a) 100 pole figure of Ag twins with crystallographic orientation close to the 111 twin plane. b) Color-coded map of two  $180^\circ$  rotational twins. c) Back scattered scanning electron image obtained after FIB shaving; the white rectangle indicates the region from where the OI map was taken.

These results confirm that the growth direction of the main stem of the dendrite was close to  $[1\bar{1}2]$  and the directions of the branches were  $[1\bar{2}1]$  and  $[\bar{2}11]$ . These results clearly show that, besides the commonly accepted presence of a twin plane parallel to the broad dendrite surface plane,<sup>28,29</sup> this silver dendrite structure was characterized by the presence of two types of twins, related to each other by  $180^\circ$  rotation around the [111] crystallographic direction, as indicated in the 100 pole figure (Fig. 4a). From the color-coded map (Fig. 4b), taken from the region shown by the white rectangle in the back-scattered scanning electron image in Fig. 4c, it appears that the  $180^\circ$  rotational twin domains were randomly distributed. Colors of the twins in stereographic projection (Fig. 4a) correspond to the appropriate twin variances in the color-coded map (Fig. 4b). Not all details shown in Fig. 4c are present in the color-coded map. Since the map was obtained at a  $70^\circ$  tilt angle, any closely spaced branches, shown in Fig. 4c, cannot be separated. Both twin domains are random in terms of size and shape, and the 111 pole in the center of the 100 pole figure confirms that they

have the same (111) plane parallel to the main broad twin surface in common. High susceptibility for twinning of these dendrites comes from very low stacking fault energy of silver of  $\approx 16 \text{ mJ m}^{-2}$ .<sup>33</sup>

In summary, the structures of electrodeposited Ag dendrites were investigated by SEM, Z-contrast HAADF and OIM. The results revealed that the Ag dendrites exhibited the presence of well-defined randomly distributed twin domains of irregular size and shape. These twin domains were related to each other by  $180^\circ$  rotation around the common [111] crystallographic axis, which is normal to the main broad dendrite surface. The growth direction of the main dendrite stem was found to be close to  $[\bar{1}\bar{1}2]$  and the direction of the branches were  $[1\bar{2}1]$  and  $[\bar{2}11]$ .

*Acknowledgements.* V.R.R. acknowledges support by the Ministry of Education, Science and Technological Development of the Republic of Serbia, under contract No. 172054. Electron microscopy was performed at the National Center for Electron Microscopy, which is supported by the Office of Science, Office of Basic Energy Sciences, of the U.S. Department of Energy under Contract No. DE-AC02-05CH11231.

#### ИЗВОД

#### ПРОИЗВОЉНО ОРИЈЕНТИСАНИ ДОМЕНИ ДВОЈНИКА У ЕЛЕКТРОХЕМИЈСКИ ИСТАЛОЖЕНИМ ДЕНДРИТИМА СРЕБРА

ЕВИЦА Р. ИВАНОВИЋ<sup>1</sup>, НЕБОЈША Д. НИКОЛИЋ<sup>2</sup> и ВЕЛИМИР Р. РАДМИЛОВИЋ<sup>3</sup>

<sup>1</sup>Пољопривредни факултет, Универзитет у Београду, Немањина 6, Београд-Земун, <sup>2</sup>ИХТМ – Центар за електрохемију, Универзитет у Београду, Његошева 12, Београд и <sup>3</sup>Технолошки-међалуришки факултет, Универзитет у Београду, Карнејијева 4, Београд

Дендрити сребра припремљени су поступком електрохемијског таложења. Испитивани су структура, тип двојника и њихова расподела коришћењем скенирајуће електронске микроскопије (SEM), високо-угаоне трансмисионе електронске микроскопије тамног поља са контрастом атомског броја (HAADF) и кристалографски осетљиве оријентационе микроскопије (OIM). Резултати су показали да дендрите сребра карактерише присуство произвољно распоређених двојникованих домена, међусобно ротираних за  $180^\circ$  око заједничког кристалографског правца [111]. Основна фронтална раван дендрита је {111} типа. Главно стабло дендрита и све дендритне гране расту у кристалографским правцима типа <112>.

(Примљено 6. марта, ревидирано 16. априла, прихваћено 18. априла 2014)

#### REFERENCES

1. J. S. Langer, *Rev. Mod. Phys.* **52** (1980) 1
2. E. Ben-Jacob, P. Garik, *Nature* **343** (1990) 523
3. M. C. Cross, P. C. Hohenberg, *Rev. Mod. Phys.* **65** (1993) 851
4. S. Xie, X. Zhang, D. Xiao, M. C. Paau, J. Huang, M. M. F. Choi, *J. Phys. Chem., C* **115** (2011) 9943
5. Z. Zheng, S. C. Tang, S. Vongehr, X. K. Meng, *Mater. Chem. Phys.* **129** (2011) 594
6. M. H. Rashid, T. K. Mandal, *J. Phys. Chem., C* **111** (2007) 16750
7. X. Qin, H. Wang, X. Wang, Z. Miao, Y. Fang, Q. Chen, X. Shao, *Electrochim. Acta* **56** (2011) 3170

8. X. Wen, Y. Xie, M. W. C. Mak, K. Y. Cheung, X. Li, R. Renneberg, S. Yang, *Langmuir* **22** (2006) 4836
9. C. Gu, T. Y. Zhang, *Langmuir* **24** (2008) 12010
10. K. I. Popov, S. S. Djokić, B. N. Grgur, *Fundamental Aspects of Electrometallurgy*, Kluwer Academic/Plenum Publishers, New York, 2002, pp. 1–305
11. Z. Jiang, Y. Lin, Z. Xie, *Mat. Chem. Phys.* **134** (2012) 762
12. Q. Zhou, B. Wang, P. Wang, C. Dellago, Y. Wang, Y. Fang, *CrystEngCom.* **15** (2013) 5114
13. J. Zhu, S. Liu, O. Palchik, Y. Koltypin, A. Gedanken, *Langmuir* **16** (2000) 6396
14. Y. Socol, O. Abramson, A. Gedanken, Y. Meshorer, L. Berenstein, A. Zaban, *Langmuir* **18** (2002) 4736
15. R. He, X. Qian, J. Yin, Z. Zhu, *Chem. Phys. Lett.* **369** (2003) 454
16. S.-D. Wu, Z. Zhu, Z. Zhang, L. Zhang, *J. Chem. Res.* **2002** (2002) 342
17. Z. Wang, F. Tao, D. Chen, L. Yao, W. Cai, X. Li, *Chem. Lett.* **36** (2007) 672
18. T. A. Witten, L. M. Sander, *Phys. Rev. Lett.* **47** (1981) 1400
19. J. X. Fang, H. J. You, P. Kong, Y. Yi, X. P. Song, B. J. Ding, *Cryst. Growth. Des.* **7** (2007) 864
20. Y. C. Han, S. H. Liu, M. Han, J. C. Bao, Z. H. Dai, *Cryst. Growth. Des.* **9** (2009) 3941
21. R. L. Penn, J. F. Banfield, *Science* **281** (1998) 969
22. G. X. Zhang, S. H. Sun, M. N. Banis, R. Y. Li, M. Cai, X. L. Sun, *Cryst. Growth. Des.* **11** (2011) 2493
23. H. P. Ding, G. Q. Hin, K. C. Chen, M. L. Zhang, Q. Y. Liu, J. C. Hao, H. G. Liu, *Colloids Surfaces, A* **353** (2010) 166
24. M. A. Meyers, L. E. Murr, *Acta Met.* **26** (1978) 951
25. S. Hayashi, R. Koga, M. Ohtuji, K. Yamamoto, M. Fujii, *Solid State Commun.* **76** (1990) 1067
26. W. W. Mullins, R. F. Sekerka, *J. Appl. Phys.* **35** (1964) 444
27. J. L. Barton, J. O'M. Bockris, *Proc. Roy. Soc., A* **268** (1962) 485
28. R. S. Wagner, *Acta Met.* **8** (1960) 57
29. D. R. Hamilton, R. G. Seidensticker, *J. Appl. Phys.* **31** (1960) 1165
30. J. K. Farrer, M. C. Chipman, M. Tiner, *Microsc. Microanal.* **8** (2002) 544 CD
31. T. L. Matteson, S. W. Schwartz, E. C. Houge, B. W. Kempshall, L. A. Gianuzzi, *J. Electronic. Mater.* **31** (2002) 33
32. G. Wranglen, *Electrochim. Acta* **2** (1960) 130
33. R. E. Smallman, R. J. Bishop, *Modern Physical Metallurgy and Materials Engineering*, Butterworth-Heinemann, Oxford, 1999, p. 101.